

8 Phase transitions, thermal transport and new materials

A. Schilling, M. Reibelt, and R. DellAmore

in collaboration with:

Paul Scherrer Institute (Ch. Rüegg), University of Bern (K. Krämer), Bhaba Atomic Research Center (G. Ravikumar), Forschungszentrum Karlsruhe (Th. Wolf, C. Meingast), Iowa State University (P. Canfield), ETH Zürich (J. Karpinski).

In our new research group that started activity in April 2003 we are mainly investigating phase transitions, thermal transport, and the physical properties of new materials.

The study of phase transitions of vortex matter in conventional and high-temperature superconductors is a continuation of our work that we have done at the University of Karlsruhe (Germany). The physics of magnetic flux lines (vortices) in high-temperature superconductors has been a matter of very active research because of its high relevance for the technical applications of these materials [1]. Details in the magnetic phase diagrams of the vortex lattices in other classes of type-II superconductors have also become of growing interest [2; 3; 4]. However, no thermodynamic data on the different vortex phases and respective phase transitions in these systems are available. There are possibilities to circumvent known problems associated with vortex pinning [5; 6], and it is therefore likely that corresponding experiments will eventually be successful.

The main mechanisms for the transport of heat in simple three dimensional solids are quite well understood, and the corresponding contributions to the thermal conductivity by lattice vibrations (phonons) and nearly-free electrons in simple metals are standard subjects in all solid-state physics textbooks. By contrast, little is known about the mechanism for the heat transport in lower dimensional systems. The application of theoretical microscopic models for the heat transport in one and two dimensional atomic lattices, for example, gives surprising results. Fourier's law is expected to be violated in reduced dimensions, and the thermal conductivity should diverge with increasing system size [7; 8]. There are indeed a variety of real systems, where such deviations from standard three dimensional phonon heat transport can be expected, and we aim to perform thermal-conductivity experiments on such systems.

- [1] G. Blatter *et al.*, Rev. Mod. Phys. **66**, 1125 (1994).
- [2] V.G. Kogan *et al.*, Phys.Rev.B **55**, R8693.
- [3] M.R. Eskildsen *et al.*, Phys.Rev.Lett.**78**, 1968 (1997).
- [4] C.E. Sosolik *et al.*, Phys.Rev.B **68**, 140503 (2003).
- [5] M. Willemin *et al.*, Phys.Rev.B **58**, R5940 (1998).
- [6] E.H. Brandt and G.P. Mikitik, Phys.Rev.Lett.**89**, 027002 (2002).
- [7] A. Lippi and R. Livi, J. Stat. Phys. **100**, 1147 (2000).
- [8] O. Narayan and S. Ramaswamy, Phys.Rev.Lett.**89**, 200601 (2002).

8.1 Phase transitions in superconductors

8.1.1 Magnetocaloric effects and vortex phases in V_3Si

The magnetic phase diagram of the type-II superconductor V_3Si in the superconducting state has been previously studied by DC magnetisation measurements. In external magnetic fields in the mixed

state above $\mu_0 H = 1$ T, the magnetisation M shows a pronounced hysteretic peak effect that defines two distinct magnetic fields: the peak field B_P where the hysteresis width is largest, and the onset field B_{HF} where the large peak in the hysteresis loop opens (see Fig. 8.1, upper figures). This onset has been shown to depend on the magnetic history of the sample and is sharpest after repeated fields cycles below B_{HF} . The magnetic region right below B_{HF} is believed to exhibit long-range order of the vortex lattice, while the peak region very likely corresponds to a disordered glass-like state.

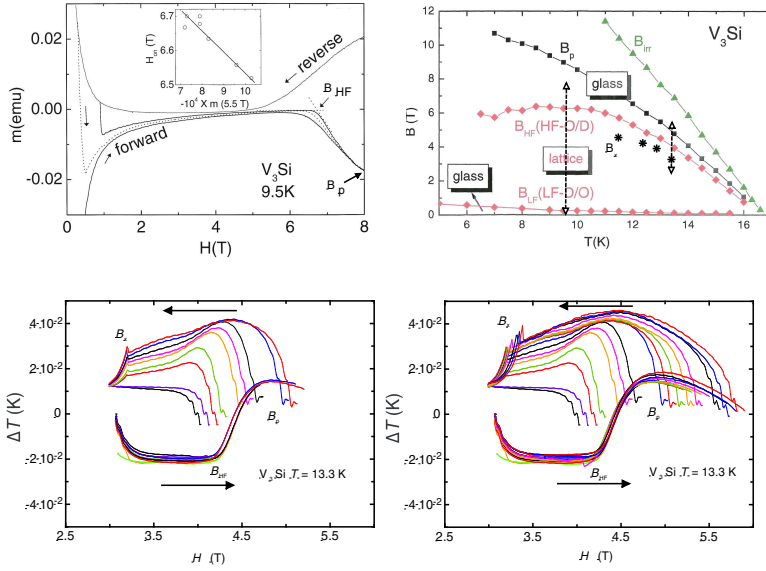


Figure 8.1: Phase diagram and magnetocaloric effect in V_3Si (see text).

rounding heat reservoir, $\frac{dH}{dt}$ is the rate of the field variation, and C is the sample heat capacity. In such an experiment, the thermodynamic quantity $(\frac{\partial M}{\partial T})_H$ is probed, which is usually inaccessible in magnetisation experiments due to the large hysteresis effects on M .

We have performed numerous experiments by varying the magnetic history of the sample below B_{HF} . We could not detect any feature that would indicate a thermodynamic phase transition at B_{HF} within the resolution of the experiment. However, we have measured a large self-heating effect as soon as the magnetic field enters the peak region from below, which we interpret as the onset of a dissipative process that reflects the destruction of the long-range ordered vortex lattice. Cycling the magnetic field back to low fields is again a dissipative process, and the amount of the produced heating power depends on the width of the magnetic loop. In addition, a distinct, first-order like feature develops at a field B_x , where an approximately constant amount of heat is suddenly released, leading to an immediate increase in sample temperature (see Fig. 8.1, lower figures). This field B_x does not depend on the magnetic history as long as the backward magnetic cycles start below B_P . Cycling down from a field above this peak value, however, results in a history dependence of the location of the heat-releasing field B_x . We believe that in a small magnetic-field cycle, starting at low fields and entering the peak region at B_{HF} but reversing the sign of $\frac{dH}{dt}$ below B_P , a metastable and perhaps incomplete glassy state is established in the peak region that discontinuously transforms back to a regular ordered solid at a well defined magnetic field B_x by releasing a finite amount of heat. Larger cycles that exceed the peak field B_P seem to produce disordered vortex configurations that transform back at different transformation fields B_x , depending on the width of the respective cycles.

These investigations show that a variety of thermal effects in V_3Si can be ascribed to the formation of different vortex phases. Most of these phases are not in thermodynamic equilibrium. To study these

We have investigated the magnetic phase diagram of V_3Si using a differential calorimeter to detect possible thermodynamic phase transition between the different vortex phases. Our main result is shown in Fig. 8.1 (lower figures), where we have plotted the magnetocaloric effect on the sample temperature T in a differential setup with finite heat links. In the steady state, the temperature difference ΔT to a copper reference sample corresponds, to first approximation, to the variation of $\tau \frac{dH}{dt} (\frac{\partial M}{\partial T})_H \frac{T}{C}$ of V_3Si , where τ is the thermal relaxation time of the sample due to the finite heat link to the sur-

glass-like phases in more detail we are now using external transverse AC-field coils that have been shown to be effective to drive non-equilibrium vortex states into a thermodynamic equilibrium [1; 2].

8.1.2 The effect of twin-boundary and intrinsic pinning on flux-lattice melting in single crystals of $REBa_2Cu_3O_{7-\delta}$ ($RE = Y, Nd$)

Some characteristic features of high-temperature superconductors, such as the magnetic-field-broadened resistive transition, have made pinning a central issue in the study of these materials. The presence of a melting transition for $H//c$ in untwinned $YBa_2Cu_3O_{7-\delta}$ crystals, in contrast to its absence in twinned crystals at low magnetic fields, indicates that twin boundaries play a major role in determining the vortex structure and its dynamics for this magnetic field orientation. Measurements of the magnetization on $YBa_2Cu_3O_{7-\delta}$ [3] and $NdBa_2Cu_3O_{7-\delta}$ [4] and transport measurements on $YBa_2Cu_3O_{7-\delta}$ [5] have indicated that for $H//ab$, strong commensurability effects between the vortex lattice and the crystal lattice occur, and the phase-transition line separating the vortex solid from the vortex liquid can be expected to strongly deviate from continuum-theory expectations. In fact an oscillatory melting temperature of the vortex smectic phase as a function of magnetic field has been measured by [3; 4; 5].

Every inhomogeneity of the material that weakens superconductivity can cause pinning. Pinning centers are, for example, grain boundaries, twin boundaries, dislocations, impurities and even the crystal structure itself in the case of layered superconductors. When the magnetic field is applied parallel to the superconducting CuO_2 -planes in cuprates, Josephson vortices can form, with their axes along the weakly superconducting intermediate layers. These intermediate layers are effective pinning centers with respect to vortex motion perpendicular to the planes, but the vortices are still able to easily move parallel to the layers. This behaviour reminds of a smectic liquid crystal phase and is therefore called "vortex smectic phase". This phenomenon causes commensurability between the vortex lattice and the layered crystal structure when the condition $l = kd$ is satisfied [6; 7]. Here k is an integer number, $l = [\sqrt{3}\phi_0/(2\gamma B)]^{1/2}$ is the vortex distance along the c axis, and γ is the anisotropy parameter. The oscillations in the melting temperature as a function of magnetic field are a direct consequence of the difference between the confinement strengths in commensurate and incommensurate smectic vortex states. The commensurate states experience a stronger confinement potential and hence melt at higher temperatures than the incommensurate states. Figure 8.2 shows possible arrangements of the vortices in different commensurate and incommensurate states.

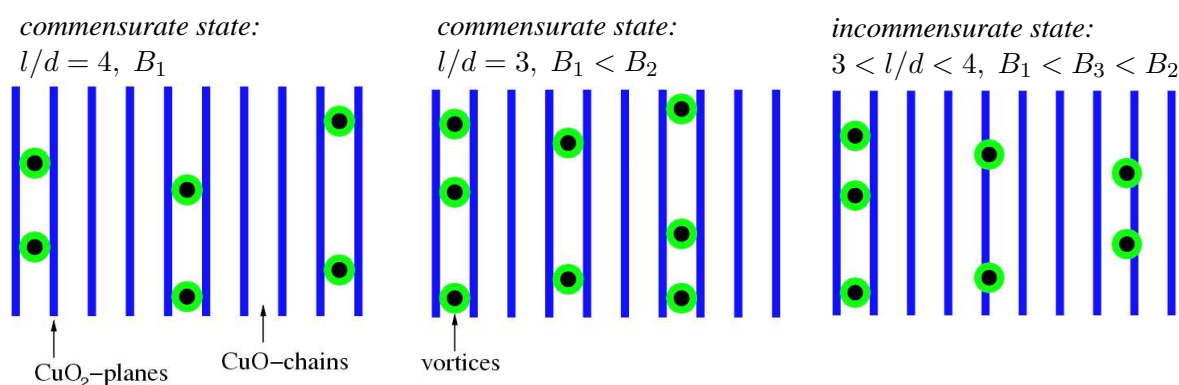


Figure 8.2: Possible arrangements of the vortices in different commensurate and incommensurate states (see text).

We have done a series of experiments to investigate these commensurability oscillations of the melting transition by specific-heat measurements, which has not been carried out before. Transport measurements indicated that the freezing of the vortex liquid into a smectic phase is a first-order transition, but a final confirmation requires measurements of thermodynamic quantities. We first investigated a twinned $\text{NdBa}_2\text{Cu}_3\text{O}_{7-\delta}$ ($T_c \approx 96.8$ K) single crystal. We used a high-accuracy differential thermal analysis (DTA) method [8], and attached a small laser-setup on the rotation axis to achieve a high angular resolution. Although we used the same single crystals as in [4], our experiments indicated that the pinning due to the strong twinning of the crystal makes a distinction between a continuous glass-to-liquid transition from the predicted continuous smectic-phase-to-liquid transition for $H//ab$ very difficult.

We decided to repeat these measurements on an oxygen depleted $\text{NdBa}_2\text{Cu}_3\text{O}_{7-\delta}$ single crystal with $T_c \approx 65$ K. It is known that such crystals exhibit a relatively large electronic anisotropy, which favours the formation of a vortex smectic phase already in moderate magnetic fields [5]. However, we again did not detect any distinct signal due to the expected phase transition, which we attribute to considerable random (chemical) disorder in the considered sample, thereby reducing the difference in the effectiveness of pinning between commensurate and incommensurate vortex states.

- [1] M. Willemin *et al.*, Phys.Rev.B **58**, R5940 (1998).
- [2] E.H. Brandt and G.P. Mikitik, Phys.Rev.Lett.**89**, 027002 (2002).
- [3] A. A. Zhukov *et al.*, Phys.Rev.B **59**, 11213 (1999).
- [4] H. K upfer *et al.*, Phys.Rev.B **66**, 064512 (2002).
- [5] S. N. Gordeev *et al.*, Phys.Rev.Lett.**85**, 4594 (2000).
- [6] B. I. Ivlev and N. B. Kopnin, Phys.Rev.Lett.**64**, 1828 (1990).
- [7] L. Bulaevskii and J. R. Clem, Phys.Rev.B **44**, 10234 (1991).
- [8] A. Schilling and O. Jeandupeux, Phys.Rev.B **52**, 9714 (1995).

8.2 Thermal transport

8.2.1 Thermal-conductivity measurements on the quasi one dimensional $S = \frac{1}{2}$ quantum spin system TlCuCl_3

We performed thermal-conductivity measurements on the quantum spin system TlCuCl_3 . This material has a monoclinic structure (space group $P2_1/c$) and shows changes of the spin state, that depend on the temperature T as well as on the applied magnetic field H .

The magnetic properties are determined by the $S = \frac{1}{2}$ exchange interactions between the Cu^{2+} ions, which are arranged in dimer pairs within Cu_2Cl_6 -clusters. These planar dimers are stacked on the top of one another to form infinite double chains parallel to the crystallographic a -axis [1]. These double chains are located at the corners and the center of the unit cell in the $b - c$ plane, and are separated by Tl^+ .

The magnetic ground state of TlCuCl_3 is a non-magnetic spin singlet, that is separated from the first excited triplet state by an excitation gap $\Delta = 0.65$ meV in zero magnetic field. The magnitude of the spin gap Δ was evaluated by previous magnetization and ESR measurements [2]. Inelastic neutron-scattering measurements revealed that the spin gap is due to the strong antiferromagnetic interaction $J = 5.68$ meV in the planar dimer of Cu_2Cl_6 . The neighboring dimers are coupled by strong interdimer interactions along the double chain and in the $(1\ 0\ -2)$ plane [3; 4]. These 3D interactions play an important role concerning the quantum regime of this compound. The critical field H_c is defined as

the magnetic field corresponding to the gap energy $\Delta = g\mu_0\mu_B H_c$. When a magnetic field H larger than H_c is applied, the energy gap vanishes and the system can undergo a three dimensional magnetic ordering. The process of closing the spin excitation gap drives a quantum phase transition, which separates the quantum disordered singlet ground state from the 3D ordered ground state. The critical field for TlCuCl_3 is $\mu_0 H_c \approx 5.5$ T at $T = 0$ K [2]. The ordering temperature increases with increasing magnetic field for $H > H_c$. These features were interpreted and qualitatively well described in terms of the Bose-Einstein condensation (BEC) of spin triplets (magnons) [5]. The coherent superposition of the singlet and the $S_z = +1$ triplet components throughout the Cu^{2+} -dimers generates the condensate (S_z denotes the the quantum number for the spin component along the quantization axis) [6]. The spin structure in the ordered state has been determined by elastic neutron-scattering measurements. The spins lie in the $a - c$ plane, with $H \parallel b$. They are arranged in parallel along a leg in the double chain and form an angle $\alpha = 39^\circ$ with the a -axis. The transverse spin components are long-range ordered [7].

Our thermal-conductivity measurements are motivated by the above mentioned quantum phase transition and the possibility to detect thermal signatures due to the presence of a Bose-Einstein condensate. We measured the thermal conductivity with a conventional steady state method along the crystallographic a -axis, and applying a magnetic field H up to $\mu_0 H = 9$ T along the direction of the heat flux $\parallel a$. An enhancement of κ at lower temperatures is observable (see Fig. 8.3). With increasing magnetic field the absolute values of κ decrease in this temperature region. At higher temperatures the thermal conductivity is magnetic field independent. Further measurements of the thermal conductivity along other directions, especially along and perpendicular to the ordered spin vectors, are planned.

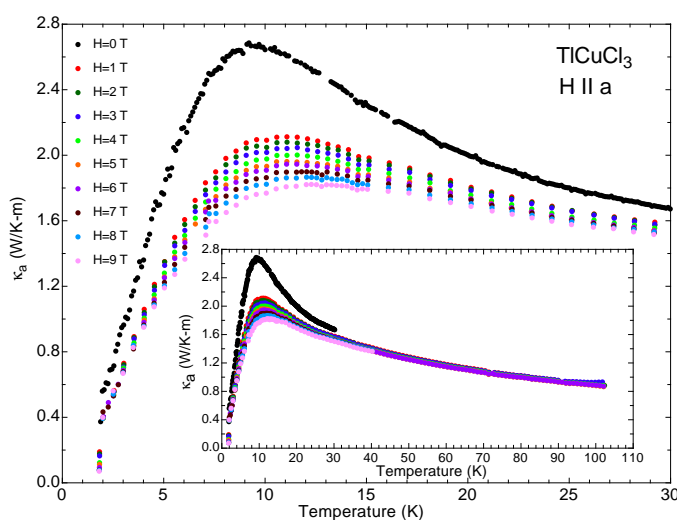


Figure 8.3: *The thermal conductivity of TlCuCl_3 along the crystallographic a -axis. The inset shows an extended temperature range.*

- [1] K. Takatsu *et al.*, J. Phys. Soc. Jpn. **66**, 1611 (1997).
- [2] A. Oosawa *et al.*, J. Phys.: Condens. Matter. **11**, 265 (1999).
- [3] N. Cavadini *et al.*, Phys.Rev.B **63**, 172414 (2001).
- [4] A. Oosawa *et al.*, Phys.Rev.B **64**, 094426 (2002).
- [5] T. Nikuni *et al.*, Phys.Rev.Lett.**84**, 5868 (2000).
- [6] Ch. Rügge *et al.*, Nature **423**, 62 (2003).
- [7] A. Oosawa *et al.*, J. Phys. Soc. Jpn. **72**, 1026 (2003).